Applied Physics Reviews

RESEARCH ARTICLE | SEPTEMBER 05 2025

Anomalous Maxwell-Garnett theory for photonic time crystals

Zheng Gong ; Ruoxi Chen ; Hongsheng Chen ; Xiao Lin

Appl. Phys. Rev. 12, 031414 (2025)
https://doi.org/10.1063/5.0275246

Applied Physics Reviews ARTICLE pubs.aip.org/aip/are

Anomalous Maxwell-Garnett theory for photonic time crystals

Cite as: Appl. Phys. Rev. **12**, 031414 (2025); doi: 10.1063/5.0275246
Submitted: 11 April 2025 · Accepted: 20 August 2025 ·
Published Online: 5 September 2025

Zheng Gong,[1,2] Ruoxi Chen,[1,2] Hongsheng Chen,[1,2,a)] and Xiao Lin[1,2,a)]

AFFILIATIONS

[1]Interdisciplinary Center for Quantum Information, State Key Laboratory of Extreme Photonics and Instrumentation, Zhejiang Key Laboratory of Intelligent Electromagnetic Control and Advanced Electronic Integration, College of Information Science & Electronic Engineering, Zhejiang University, Hangzhou 310027, China
[2]International Joint Innovation Center, The Electromagnetics Academy at Zhejiang University, Zhejiang University, Haining 314400, China

[a)]Authors to whom correspondence should be addressed: hansomchen@zju.edu.cn and xiaolinzju@zju.edu.cn

ABSTRACT

The Maxwell-Garnett theory, dating back to James Clerk Maxwell-Garnett's foundational work in 1904, provides a simple yet powerful framework to describe the inhomogeneous structure as an effective homogeneous medium, which significantly reduces the overall complexity of analysis, calculation, and design. As such, the Maxwell-Garnett theory enables many practical applications in diverse realms, ranging from photonics, acoustics, mechanics, thermodynamics, to materials science. It has long been thought that the Maxwell-Garnett theory of light in impedance-mismatched periodic structures is valid only *within* the long-wavelength limit, necessitating either the temporal or spatial period of light to be much larger than that of structures. Here, we break this long-held belief by revealing an anomalous Maxwell-Garnett theory for impedance-mismatched photonic time crystals *beyond* this long-wavelength limit. The key to this anomaly lies in the Fabry–Pérot resonance. We discover that under the Fabry–Pérot resonance, the impedance-mismatched photonic time crystal could be essentially equivalent to a homogeneous temporal slab simultaneously at specific discrete wavelengths, despite the temporal period of these light being comparable to or even much smaller than that of photonic time crystals.

INTRODUCTION

The Maxwell-Garnett theory, as the simplest effective medium theory, is well-known for its enticing capability to model the inhomogeneous structure, such as metamaterials and random media with irregular geometries, as an effective homogeneous medium.[1,2] It was first proposed for light by James Clerk Maxwell-Garnett one century ago[3,4] and later generalized to other wave systems,[5–9] including acoustic waves and water waves. According to the Maxwell-Garnett theory of light, the optical response of effective media could be formulated in a local or wavevector-independent fashion, which is solely governed by the geometrical parameters (e.g. filling ratio) and the intrinsic properties (e.g. impedance) of each constituent material. This mathematical simplification and physical elegance significantly reduce the computational cost and complexity, which would otherwise be computationally prohibitive, and further make the Maxwell-Garnett theory feasible to perform accurate analysis and design for intricate inhomogeneous structures with desired properties that are hard or even impossible to find in nature.[10–13] Therefore, the Maxwell-Garnett theory of light could greatly facilitate the flexible manipulation of light-matter interactions and is of fundamental importance to many practical applications, ranging from hyperlenses, metalenses, invisibility cloak, super-scatterers, to absorbers.[14–18]

Despite the long research history of effective medium theory,[19–26] it is widely believed that the local Maxwell-Garnett theory of light would break down for impedance-mismatched periodic structures beyond the long-wavelength limit. The underlying reason is that when the spatial or temporal period of light is comparable to or much smaller than that of structures, the effective medium theory generally needs to be reformulated into a nonlocal or wavevector-dependent fashion, in order to incorporate the influence of high-order scattering of light.[27–31] The resultant nonlocal effective medium theory is much more complicated and accurate than the local Maxwell-Garnett theory, but it oftentimes loses the practical convenience for the straightforward analysis and design of complex structures. In 1988, Ref. 25 found that the local Maxwell-Garnett theory can perform well beyond the long-wavelength limit for spatially inhomogeneous structures, via impedance matching at the Brewster angle. Recently, this finding was generalized to impedance-matched temporally inhomogeneous photonic time crystals.[26]

Here, we reveal a universal mechanism to enable the anomalous local Maxwell-Garnett theory for impedance-mismatched photonic time crystals beyond the long-wavelength limit, which breaks the above century-old belief. This anomalous Maxwell-Garnett theory is essentially attributed to the Fabry–Pérot resonance. Since the Fabry–Pérot resonance condition can be readily achieved through the structural design, without any fundamental structural limitation (e.g. temporal period of photonic time crystals[32–41]) and any fundamental material limitation (e.g. impedances of constituent materials), our revealed mechanism for the anomalous Maxwell-Garnett theory circumvents the critical requirement for photonic time crystals being either within the long-wavelength limit or impedance-matched. Therefore, our finding further develops the conventional Maxwell-Garnett theory and might be crucial to the continuous exploration of temporal or spatiotemporal media.[42–51]

RESULTS

We begin with the introduction of the Maxwell-Garnett theory for photonic time crystals in Fig. 1. Without loss of generality, the photonic time crystal is homogeneous in space but has a time period T_{PTC} and a temporal interface number N, where $N=\infty$ without specific specification, and it is composed of two constituent media in Fig. 1(a). The constituent medium X (X = I or II) has the temporal filling ratio $\tau_{\mathrm{X}}/T_{\mathrm{PTC}}$, the permittivity ε_{X}, the permeability μ_{X}, and the impedance $\eta_{\mathrm{X}}=\sqrt{\mu_{\mathrm{X}}/\varepsilon_{\mathrm{X}}}$, where $T_{\mathrm{PTC}}=\tau_{\mathrm{I}}+\tau_{\mathrm{II}}$. According to the Bloch band theory, the dispersion relation of photonic time crystals can be analytically obtained as[52]

$$\cos(\omega_{\mathrm{PTC}}\cdot T_{\mathrm{PTC}})=\cos(\omega_{\mathrm{I}}\tau_{\mathrm{I}})\cos(\omega_{\mathrm{II}}\tau_{\mathrm{II}})-\frac{1}{2}\left(\frac{\eta_{\mathrm{I}}}{\eta_{\mathrm{II}}}+\frac{\eta_{\mathrm{II}}}{\eta_{\mathrm{I}}}\right)\sin(\omega_{\mathrm{I}}\tau_{\mathrm{I}})\sin(\omega_{\mathrm{II}}\tau_{\mathrm{II}}),\quad (1)$$

where ω_{PTC} is the eigenfrequency of light inside the photonic time crystal, the wavevector $k=|\bar{k}|>0$ is a conservable quantity due to the momentum conservation in temporal media,[53] and $\omega_{\mathrm{X}}=k/\sqrt{\mu_{\mathrm{X}}\varepsilon_{\mathrm{X}}}$ is the angular frequency of light in medium X.

When the local Maxwell-Garnett theory works, the designed photonic time crystal could, in principle, be effectively modeled as a homogeneous temporal medium with the permittivity $\varepsilon_{\mathrm{MG}}$ and the permeability μ_{MG} in Fig. 1(b). Correspondingly, for the incident light with a given wavevector k, the eigenfrequency $\omega_{\mathrm{MG}}=2\pi/T_{\mathrm{MG}}=k/\sqrt{\mu_{\mathrm{MG}}\varepsilon_{\mathrm{MG}}}$ of light predicted by the Maxwell-Garnett theory should be equal to the eigenfrequency ω_{PTC} calculated by the Bloch band theory, namely, $\omega_{\mathrm{MG}}=\omega_{\mathrm{PTC}}$, where T_{MG} essentially corresponds to the temporal period of incident light. By substituting $\omega_{\mathrm{MG}}=\omega_{\mathrm{PTC}}$ into Eq. (1), we further have

$$\begin{aligned}\cos(\omega_{\mathrm{MG}}\cdot T_{\mathrm{PTC}})&=\cos(2\pi\cdot T_{\mathrm{PTC}}/T_{\mathrm{MG}})\\&=\cos(\omega_{\mathrm{I}}\tau_{\mathrm{I}})\cos(\omega_{\mathrm{II}}\tau_{\mathrm{II}})\\&\quad-\frac{1}{2}\left(\frac{\eta_{\mathrm{I}}}{\eta_{\mathrm{II}}}+\frac{\eta_{\mathrm{II}}}{\eta_{\mathrm{I}}}\right)\sin(\omega_{\mathrm{I}}\tau_{\mathrm{I}})\sin(\omega_{\mathrm{II}}\tau_{\mathrm{II}}).\end{aligned}\quad (2)$$

Upon close inspection of Eq. (2), it might be simplified under three distinct conditions, which directly leads to the emergence to three distinct types of local Maxwell-Garnett theories.

For type 1, when $\omega_{\mathrm{MG}}T_{\mathrm{PTC}}=2\pi\cdot T_{\mathrm{PTC}}/T_{\mathrm{MG}}\to 0$ and $\omega_{\mathrm{X}}\tau_{\mathrm{X}}\to 0$, the incident light is within the long-wavelength limit. When within this long-wavelength limit, the Taylor expansion is applicable to Eq. (2), namely, $\cos(\omega_{\mathrm{MG}}T_{\mathrm{PTC}})\approx 1-(\omega_{\mathrm{MG}}T_{\mathrm{PTC}})^2/2$, $\cos(\omega_{\mathrm{X}}\tau_{\mathrm{X}})\approx 1-(\omega_{\mathrm{X}}\tau_{\mathrm{X}})^2/2$, and $\sin(\omega_{\mathrm{X}}\tau_{\mathrm{X}})\approx\omega_{\mathrm{X}}\tau_{\mathrm{X}}$. This way, after some calculations, Eq. (2) can be reduced to

$$\frac{T_{\mathrm{PTC}}}{\mu_{\mathrm{MG}}}\cdot\frac{T_{\mathrm{PTC}}}{\varepsilon_{\mathrm{MG}}}=\left(\frac{\tau_{\mathrm{I}}}{\mu_{\mathrm{I}}}+\frac{\tau_{\mathrm{II}}}{\mu_{\mathrm{II}}}\right)\cdot\left(\frac{\tau_{\mathrm{I}}}{\varepsilon_{\mathrm{I}}}+\frac{\tau_{\mathrm{II}}}{\varepsilon_{\mathrm{II}}}\right).\quad (3)$$

Accordingly, one possible solution to Eq. (3) is

$$\left.\begin{aligned}\frac{T_{\mathrm{PTC}}}{\varepsilon_{\mathrm{MG}}}&=\frac{\tau_{\mathrm{I}}}{\varepsilon_{\mathrm{I}}}+\frac{\tau_{\mathrm{II}}}{\varepsilon_{\mathrm{II}}}\\\frac{T_{\mathrm{PTC}}}{\mu_{\mathrm{MG}}}&=\frac{\tau_{\mathrm{I}}}{\mu_{\mathrm{I}}}+\frac{\tau_{\mathrm{II}}}{\mu_{\mathrm{II}}}\end{aligned}\right\},\quad \text{if within the long–wavelength limit (including } \omega_{\mathrm{MG}}T_{\mathrm{PTC}}\to 0).\quad (4)$$

Equation (4) is exactly the conventional Maxwell-Garnett mixing formulas,[1,2] widely known for temporal media.[21] Generally, this conventional Maxwell-Garnett theory governed by Eq. (4) can obtain $\omega_{\mathrm{MG}}=\omega_{\mathrm{PTC}}$ (or more precisely speaking, $\omega_{\mathrm{MG}}\approx\omega_{\mathrm{PTC}}$) only within the long-wavelength limit, as shown in Figs. 2(a) and 2(b), where $\varepsilon_{\mathrm{I}}/\varepsilon_0=1$, $\varepsilon_{\mathrm{II}}/\varepsilon_0=8.9$, and $\mu_{\mathrm{I}}/\mu_0=\mu_{\mathrm{II}}/\mu_0=1$ are used in Fig. 2(b) and ε_0 and μ_0 are the vacuum permittivity and permeability, respectively. Without further specification, $\tau_{\mathrm{I}}/T_{\mathrm{PTC}}=\tau_{\mathrm{II}}/T_{\mathrm{PTC}}=0.5$.

For type 2, when $\eta_{\mathrm{I}}=\eta_{\mathrm{II}}$, the designed photonic time crystal is impedance-matched. Accordingly, the impedance $\eta_{\mathrm{MG}}=\sqrt{\mu_{\mathrm{MG}}/\varepsilon_{\mathrm{MG}}}$ of effective temporal medium is the same as that of each constituent material, namely, $\eta_{\mathrm{MG}}=\eta_{\mathrm{I}}=\eta_{\mathrm{II}}$. By substituting this impedance-matching condition into Eq. (2), Eq. (2) can be simplified to $\cos(\omega_{\mathrm{MG}}\ T_{\mathrm{PTC}})=\cos(\omega_{\mathrm{I}}\tau_{\mathrm{I}})\cos(\omega_{\mathrm{II}}\tau_{\mathrm{II}})-\sin(\omega_{\mathrm{I}}\tau_{\mathrm{I}})\sin(\omega_{\mathrm{II}}\tau_{\mathrm{II}})=\cos(\omega_{\mathrm{I}}\tau_{\mathrm{I}}+\ \omega_{\mathrm{II}}\tau_{\mathrm{II}})$. This way one simple solution to Eq. (2) is $\omega_{\mathrm{MG}}T_{\mathrm{PTC}}=\omega_{\mathrm{I}}\tau_{\mathrm{I}}+\omega_{\mathrm{II}}\tau_{\mathrm{II}}$, namely,

$$\frac{T_{\mathrm{PTC}}}{\sqrt{\mu_{\mathrm{MG}}\varepsilon_{\mathrm{MG}}}}=\frac{\tau_{\mathrm{I}}}{\sqrt{\mu_{\mathrm{I}}\varepsilon_{\mathrm{I}}}}+\frac{\tau_{\mathrm{II}}}{\sqrt{\mu_{\mathrm{II}}\varepsilon_{\mathrm{II}}}}.\quad (5)$$

By combining the impedance-matching condition and Eq. (5), we further have

$$\left.\begin{aligned}\frac{T_{\mathrm{PTC}}}{\varepsilon_{\mathrm{MG}}}&=\frac{\tau_{\mathrm{I}}}{\varepsilon_{\mathrm{I}}}+\frac{\tau_{\mathrm{II}}}{\varepsilon_{\mathrm{II}}}\\\frac{T_{\mathrm{PTC}}}{\mu_{\mathrm{MG}}}&=\frac{\tau_{\mathrm{I}}}{\mu_{\mathrm{I}}}+\frac{\tau_{\mathrm{II}}}{\mu_{\mathrm{II}}}\end{aligned}\right\},\quad \text{if } \eta_{\mathrm{I}}=\eta_{\mathrm{II}},\ \text{for}\ \forall\,\omega_{\mathrm{MG}}T_{\mathrm{PTC}}/2\pi=T_{\mathrm{PTC}}/T_{\mathrm{MG}}.\quad (6)$$

The anomalous local Maxwell-Garnett theory[26] governed by Eq. (6) is in accordance with the conventional one governed by Eq. (4), but it can now perform well and obtain $\omega_{\mathrm{MG}}=\omega_{\mathrm{PTC}}$ exactly by exploiting the impedance matching beyond the long-wavelength limit, as shown in Figs. 2(a) and 2(c), where $\varepsilon_{\mathrm{I}}/\varepsilon_0=1$, $\varepsilon_{\mathrm{II}}/\varepsilon_0=8.9$, $\mu_{\mathrm{I}}/\mu_0=1/8.9$, and $\mu_{\mathrm{II}}/\mu_0=1$ are used in Fig. 2(c).

For type 3, when $\sin(\omega_{\mathrm{I}}\tau_{\mathrm{I}})=0$ or $\sin(\omega_{\mathrm{II}}\tau_{\mathrm{II}})=0$, one constituent medium (e.g., medium I used in the calculation later) of photonic time crystals has the temporal Fabry–Pérot resonance (see also the case where both constituents satisfy Fabry–Pérot resonance in Fig. S1). Under the scenario of Fabry–Pérot resonance of medium I, the

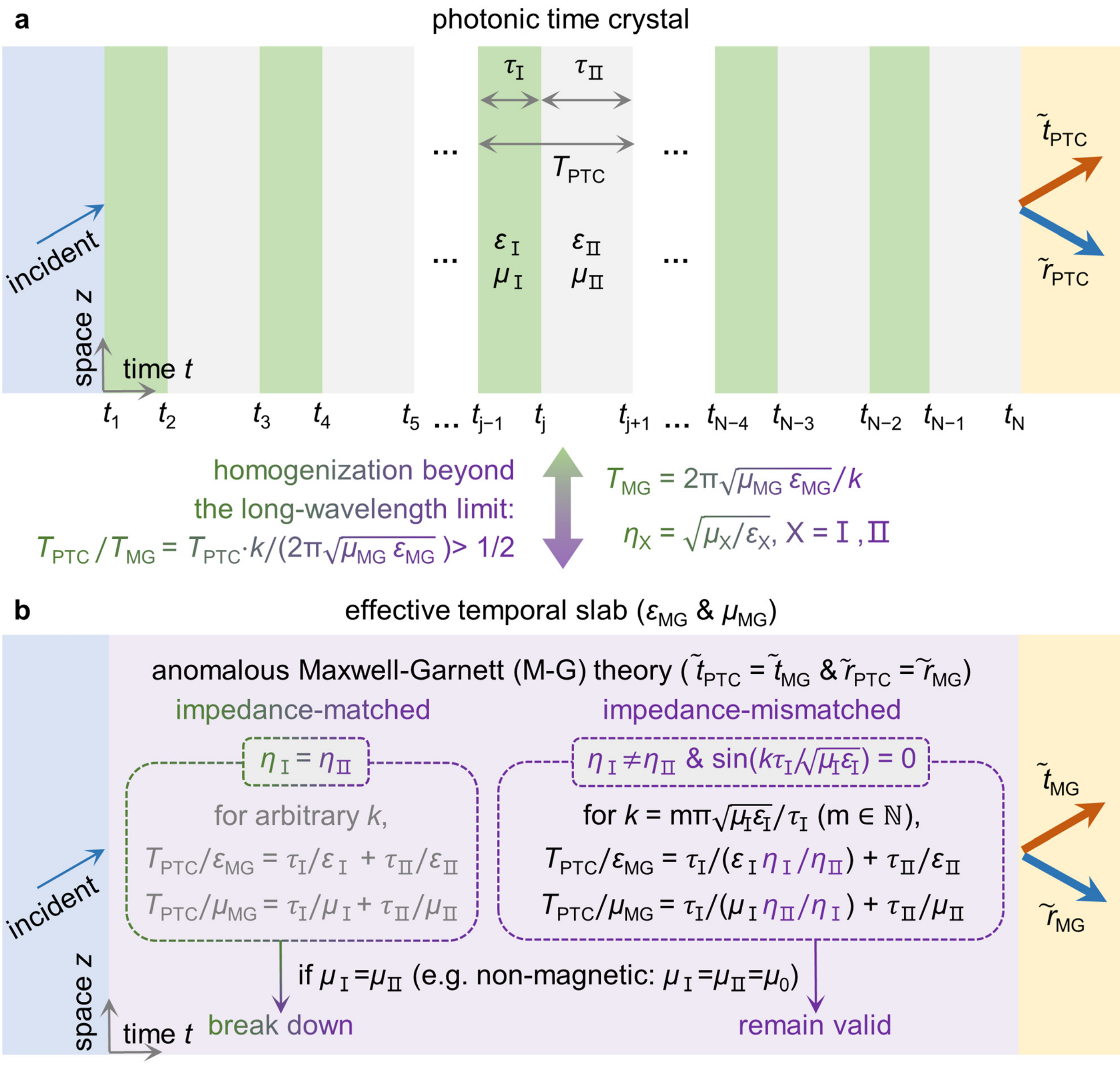

FIG. 1. Conceptual illustration of anomalous Maxwell-Garnett theory for impedance-mismatched photonic time crystals beyond the long-wavelength limit. (a) Structural schematic of a spatially homogeneous photonic time crystal with N temporal interfaces. The j-th temporal interface is created by a step change in permittivity and/or permeability at time $t = t_j$. The alternating constituent medium X (X = I or II) has a time duration τ_{X}, the permittivity ε_{X}, the permeability μ_{X}, and the wave impedance $\eta_{\mathrm{X}} = \sqrt{\mu_{\mathrm{X}}/\varepsilon_{\mathrm{X}}}$. (b) Structural schematic of the effective temporal slab homogenized via the anomalous Maxwell-Garnett theory. Beyond the long-wavelength limit, the temporal period $T_{\mathrm{MG}} = 2\pi\sqrt{\mu_{\mathrm{MG}}\varepsilon_{\mathrm{MG}}}/k$ of light predicted by the Maxwell-Garnett theory is comparable to or even smaller than the temporal period T_{PTC} of photonic time crystals, e.g., $T_{\mathrm{PTC}}/T_{\mathrm{MG}} > 1/2$, where μ_{MG} and $\varepsilon_{\mathrm{MG}}$ are the permeability and permittivity of the effective homogenized temporal slab, respectively, and k is the spatial frequency of the incident light. When the anomalous Maxwell-Garnett theory works, the transmission and reflection coefficients (i.e., $\tilde{t}_{\mathrm{PTC}}$ and $\tilde{r}_{\mathrm{PTC}}$) for the photonic time crystal are the same as those (i.e. $\tilde{t}_{\mathrm{MG}}$ and $\tilde{r}_{\mathrm{MG}}$) for the effective temporal slab, respectively, namely $\tilde{t}_{\mathrm{PTC}} = \tilde{t}_{\mathrm{MG}}$ and $\tilde{r}_{\mathrm{PTC}} = \tilde{r}_{\mathrm{MG}}$.

amplitude of light transmitting through medium I remains unchanged.[54] In other words, medium I would not contribute to the impedance of the effective temporal medium. Accordingly, the impedance η_{MG} of the effective temporal medium could be the same as the other constituent medium (i.e., medium II) of photonic time crystals, namely, $\eta_{\mathrm{MG}} = \eta_{\mathrm{II}}$. By substituting these conditions of $\sin(\omega_{\mathrm{I}}\tau_{\mathrm{I}}) = 0$ (i.e., $\cos(\omega_{\mathrm{I}}\tau_{\mathrm{I}}) = (-1)^m$ and $\omega_{\mathrm{I}}\tau_{\mathrm{I}} = m\pi$, $m \in \mathbb{N}$) and $\eta_{\mathrm{MG}} = \eta_{\mathrm{II}}$ into Eq. (2), Eq. (2) can be reduced to $\cos(\omega_{\mathrm{MG}}\,T_{\mathrm{PTC}}) = \pm\cos(\omega_{\mathrm{II}}\tau_{\mathrm{II}}) = \cos(m\pi + \omega_{\mathrm{II}}\tau_{\mathrm{II}}) = \cos(\omega_{\mathrm{I}}\tau_{\mathrm{I}} + \omega_{\mathrm{II}}\tau_{\mathrm{II}})$. This way one possible solution to Eq. (2) is $\omega_{\mathrm{MG}}T_{\mathrm{PTC}} = \omega_{\mathrm{I}}\tau_{\mathrm{I}} + \omega_{\mathrm{II}}\tau_{\mathrm{II}}$, namely,

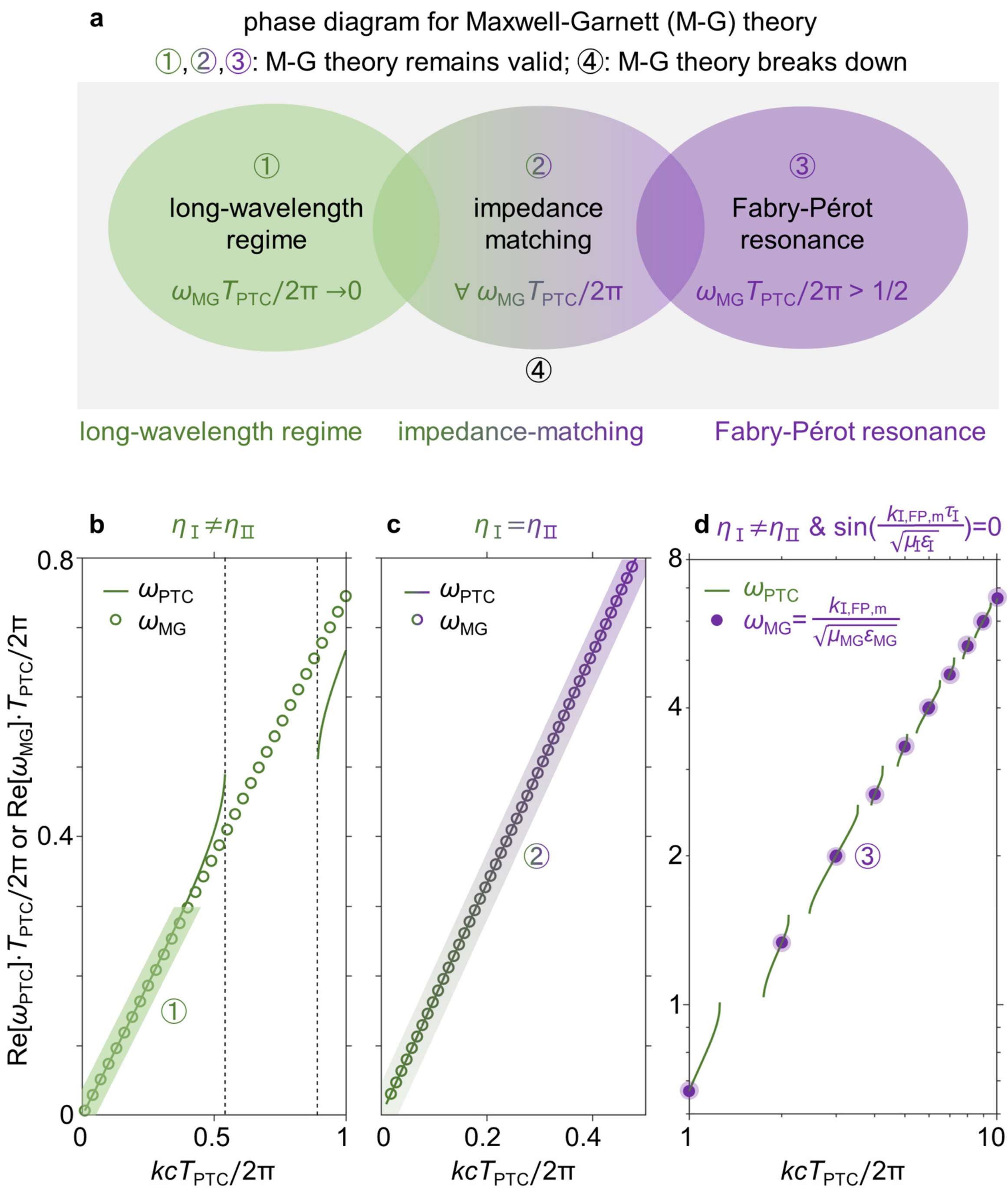

FIG. 2. Phase diagram for the Maxwell-Garnett theory. (a) Classification of conventional and anomalous Maxwell-Garnett theories. While the conventional Maxwell-Garnett theory is limited to the long-wavelength regime ① (i.e., $T_{PTC}/T_{MG} = \omega_{MG}T_{PTC}/2\pi \rightarrow 0$), the anomalous Maxwell-Garnett theory remains valid beyond the long-wavelength limit by exploiting either the impedance matching (i.e., regime ② with $\forall\, \omega_{MG}T_{PTC}/2\pi$) or the Fabry–Pérot resonance (i.e., regime ③ with $\omega_{MG}T_{PTC}/2\pi > 1/2$), where $\omega_{MG} = 2\pi/T_{MG}$ is the eigenfrequency calculated via the Maxwell-Garnett theory. In regime ④, the Maxwell-Garnett theory breaks down. (b)–(d) Band structures of photonic time crystals judiciously designed to map various Maxwell-Garnett theories in (a). While the eigenfrequency ω_{PTC} of photonic time crystals is multi-valued according to the Bloch theory, the branch cut of ω_{PTC} closest to the frequency ω_{MG} is chosen for comparison. For demonstration, $\varepsilon_I/\varepsilon_0 = 1$, $\varepsilon_{II}/\varepsilon_0 = 8.9$, and $\mu_I/\mu_0 = \mu_{II}/\mu_0 = 1$ are used in (b) and (d), while $\varepsilon_I/\varepsilon_0 = 1$, $\varepsilon_{II}/\varepsilon_0 = 8.9$, $\mu_I/\mu_0 = 1/8.9$, and $\mu_{II}/\mu_0 = 1$ are used in (c), where ε_0 and μ_0 are the vacuum permittivity and permeability, respectively, and $c = 1/\sqrt{\mu_0\varepsilon_0}$ is the light speed in vacuum. Meanwhile, we set the wavelength in vacuum $\lambda_0 = cT_0 = 500\,\mathrm{nm}$, $\tau_I/T_{PTC} = \tau_{II}/T_{PTC} = 0.5$, and the temporal period of photonic time crystals $T_{PTC} = T_0$.

$$\frac{T_{\mathrm{PTC}}}{\sqrt{\mu_{\mathrm{MG}}\varepsilon_{\mathrm{MG}}}} = \frac{\tau_{\mathrm{I}}}{\sqrt{\mu_{\mathrm{I}}\varepsilon_{\mathrm{I}}}} + \frac{\tau_{\mathrm{II}}}{\sqrt{\mu_{\mathrm{II}}\varepsilon_{\mathrm{II}}}}. \tag{7}$$

Since $\omega_{\mathrm{MG}}T_{\mathrm{PTC}} = \omega_{\mathrm{I}}\tau_{\mathrm{I}} + \omega_{\mathrm{II}}\tau_{\mathrm{II}} > \omega_{\mathrm{I}}\tau_{\mathrm{I}} = m\pi \geq \pi$, we directly have $\omega_{\mathrm{MG}}T_{\mathrm{PTC}}/2\pi = T_{\mathrm{PTC}}/T_{\mathrm{MG}} > 1/2$, indicating the temporal Fabry–Pérot resonance occurs only beyond the long-wavelength limit.

By further combining $\eta_{\mathrm{MG}} = \eta_{\mathrm{II}}$ and Eq. (7), a slightly modified but still local-form Maxwell-Garnett mixing formulas can be obtained as follows:

$$\begin{aligned} &\frac{T_{\mathrm{PTC}}}{\varepsilon_{\mathrm{MG}}} = \frac{\tau_{\mathrm{I}}}{\varepsilon_{\mathrm{I}}\eta_{\mathrm{I}}/\eta_{\mathrm{II}}} + \frac{\tau_{\mathrm{II}}}{\varepsilon_{\mathrm{II}}} \\ &\frac{T_{\mathrm{PTC}}}{\mu_{\mathrm{MG}}} = \frac{\tau_{\mathrm{I}}}{\mu_{\mathrm{I}}\eta_{\mathrm{II}}/\eta_{\mathrm{I}}} + \frac{\tau_{\mathrm{II}}}{\mu_{\mathrm{II}}}, \end{aligned} \quad \text{if } \sin(\omega_{\mathrm{I}}\tau_{\mathrm{I}}) = 0, \tag{8}$$
$$\text{for } \omega_{\mathrm{MG}}T_{\mathrm{PTC}}/2\pi = T_{\mathrm{PTC}}/T_{\mathrm{MG}} > 1/2.$$

Remarkably, this anomalous Maxwell-Garnett theory via the Fabry–Pérot resonance can obtain $\omega_{\mathrm{MG}} = \omega_{\mathrm{PTC}}$ exactly at specific discrete frequencies (i.e. $\omega_{\mathrm{MG}} = m\pi\sqrt{\mu_{\mathrm{I}}\varepsilon_{\mathrm{I}}}/(\tau_{\mathrm{I}}\sqrt{\mu_{\mathrm{MG}}\varepsilon_{\mathrm{MG}}})$) beyond the long-wavelength limit, as shown in Figs. 2(a) and 2(d), but without resorting to the impedance-matching condition. Figure 2(d) follows exactly the same structural setup as Fig. 2(b). On the other hand, the anomalous Maxwell-Garnett theory via the impedance matching always requires the existence of magnetic response, namely, either $\mu_{\mathrm{I}} \neq \mu_0$ or $\mu_{\mathrm{II}} \neq \mu_0$, and it is, thus, applicable to only magnetic photonic time crystals with $\mu_{\mathrm{I}} \neq \mu_{\mathrm{II}}$. By contrast, our revealed anomalous Maxwell-Garnett theory via the Fabry–Pérot resonance does not have any fundamental material constraint and is applicable to both magnetic and non-magnetic (i.e. $\mu_{\mathrm{I}} = \mu_{\mathrm{II}} = \mu_0$) photonic time crystals. We highlight that our revealed anomalous Maxwell-Garnett theory via the Fabry–Pérot resonance has never been discussed before.

In addition to check the criterion of $\omega_{\mathrm{MG}} = \omega_{\mathrm{PTC}}$, another criterion to examine the accuracy of Maxwell-Garnett theory is to check the equivalence between the transmission coefficient $\tilde{t}_{\mathrm{PTC}}$ (or the reflection coefficient $\tilde{r}_{\mathrm{PTC}}$) for a temporally finitely thick photonic time crystal and that ($\tilde{t}_{\mathrm{MG}}$ or $\tilde{r}_{\mathrm{MG}}$) for the effective temporal slab, namely, $\tilde{t}_{\mathrm{PTC}} = \tilde{t}_{\mathrm{MG}}$ (or $\tilde{r}_{\mathrm{PTC}} = \tilde{r}_{\mathrm{MG}}$). By following this thought, we show the relative error $\left||\tilde{t}_{\mathrm{MG}}|^2 - |\tilde{t}_{\mathrm{PTC}}|^2\right|/|\tilde{t}_{\mathrm{PTC}}|^2$ of the energy transmittivity in the $\eta_{\mathrm{I}}/\eta_{\mathrm{II}}$ - $kcT_{\mathrm{PTC}}/2\pi$ parameter space in Figs. 3(a) and 3(b), where $\varepsilon_{\mathrm{I}}/\varepsilon_0 = 1$, $\varepsilon_{\mathrm{II}}/\varepsilon_0 = 2.1$, and $\mu_{\mathrm{II}}/\mu_0 = 1$ are used in Fig. 3(a), and $\varepsilon_{\mathrm{II}}/\varepsilon_0 = 2.1$ and $\mu_{\mathrm{I}}/\mu_0 = \mu_{\mathrm{II}}/\mu_0 = 1$ are used in Fig. 3(b). For illustration, these designed photonic time crystals are surrounded by temporally semi-infinite vacuum. For magnetic photonic time crystals in Fig. 3(a), we have $\left||\tilde{t}_{\mathrm{MG}}|^2 - |\tilde{t}_{\mathrm{PTC}}|^2\right|/|\tilde{t}_{\mathrm{PTC}}|^2 \to 0$ and then $\tilde{t}_{\mathrm{PTC}} \approx \tilde{t}_{\mathrm{MG}}$ in the regime with $kcT_{\mathrm{PTC}}/2\pi = \omega_{\mathrm{MG}}T_{\mathrm{PTC}}/2\pi \cdot\sqrt{(\mu_{\mathrm{MG}}/\mu_0)(\varepsilon_{\mathrm{MG}}/\varepsilon_0)}$. The first scenario indicates that the conventional Maxwell-Garnett theory remains valid only within the long-wavelength limit, as schematically shown in Fig. 3(c). Meanwhile, we have $\left||\tilde{t}_{\mathrm{MG}}|^2 - |\tilde{t}_{\mathrm{PTC}}|^2\right|/|\tilde{t}_{\mathrm{PTC}}|^2 = 0$ and $\tilde{t}_{\mathrm{PTC}} = \tilde{t}_{\mathrm{MG}}$ in Fig. 3(a) in the regime with $\eta_{\mathrm{I}} = \eta_{\mathrm{II}}$ in Fig. 3(a), for arbitrary frequencies of incident light. The second scenario verifies the accuracy of the anomalous Maxwell-Garnett theory via the impedance matching.[26] For non-magnetic photonic time crystals in Fig. 3(b), we have $\tilde{t}_{\mathrm{PTC}} = \tilde{t}_{\mathrm{MG}}$ at a series of Fabry–Pérot resonant lines governed by $\sin(k\tau_{\mathrm{I}}/\sqrt{\mu_{\mathrm{I}}\varepsilon_{\mathrm{I}}}) = 0$ in the investigated parameter space. The third scenario essentially shows the existence of our revealed anomalous Maxwell-Garnett theory via the temporal Fabry–Pérot resonance. Remarkably, both types of anomalous Maxwell-Garnett theories could remain valid beyond the long-wavelength limit, as schematically illustrated in Fig. 3(d).

To facilitate further understanding, we show in Figs. 4(a), 4(c), and 4(e) the spatiotemporal evolution of space-time wave packets interacting with various photonic time crystals beyond the long-wavelength limit. For conceptual brevity, these designed photonic time crystals are now surrounded by temporally semi-infinite media with the permittivity $\varepsilon_{\mathrm{MG}}$ and the permeability μ_{MG}. Moreover, for the direct comparison, we also show the spatiotemporal evolution of space-time wave packets interacting with the homogenized temporal slab of each photonic time crystal in Figs. 4(b), 4(d), and 4(f). In addition, since the anomalous Maxwell-Garnett theory via the impedance matching could remain valid for arbitrary frequency of light, the incident space-time wave packet is set to follow a continuous Gaussian-type waveform in Figs. 4(c) and 4(d). Similarly, the incident space-time wave packet is set to follow a multiple-spatial harmonic waveform or a single-spatial harmonic waveform in Figs. 4(e)–4(h), since the anomalous Maxwell-Garnett theory via the temporal Fabry–Pérot resonance remains valid at specific discrete Fabry–Pérot resonant frequencies of light.

Under the judicious design in Fig. 4, there are at least two rules to follow, if the corresponding Maxwell-Garnett theory is valid. One rule is that there should be no reflection or no backward propagating light at the interface between the surrounding environment and the real photonic time crystal, when the surrounding media are set up with the effective homogenized permittivity and permeability of the photonic time crystal. The other rule to follow is that the spatiotemporal evolution of light in the temporal region (i.e., the surrounding media) behind the realistic photonic time crystal should be the same as that behind the homogenized temporal slab. The second rule does not constrain the configuration of the surrounding media (see Fig. S2, for example). According to these two rules of thumb, the conventional Maxwell-Garnett theory for conventional impedance-mismatched photonic time crystals in Figs. 4(a) and 4(b) generally breaks down beyond the long-wavelength limit. By contrast, the anomalous Maxwell theory for either the impedance-matched photonic time crystal in Figs. 4(c) and 4(d) or the impedance-mismatched photonic time crystal with the temporal Fabry–Pérot resonance in Figs. 4(e) and 4(f) remains valid beyond the long-wavelength limit.

Upon close inspection, Figs. 4(g) and 4(h) show the wave packet states before entering, traveling inside, and after exiting the impedance-mismatched photonic time crystal with the temporal Fabry–Pérot resonance. We note that the backward-propagating waves could emerge inside the photonic time crystal (the green line in the second panel), but they would further undergo the complete destructive interference (the third and fourth panels) when passing through the photonic time crystal. The deviation between the spatiotemporal evolution of light inside the realistic photonic time crystal and that inside the homogenized temporal slab should not affect the validity of Maxwell-Garnett theory.

DISCUSSION

In conclusion, we have found the existence of the anomalous Maxwell-Garnett theory for impedance-mismatched photonic time crystals beyond the long-wavelength limit by leveraging the temporal Fabry–Pérot resonance. Perhaps even more crucial is the vision emphasized

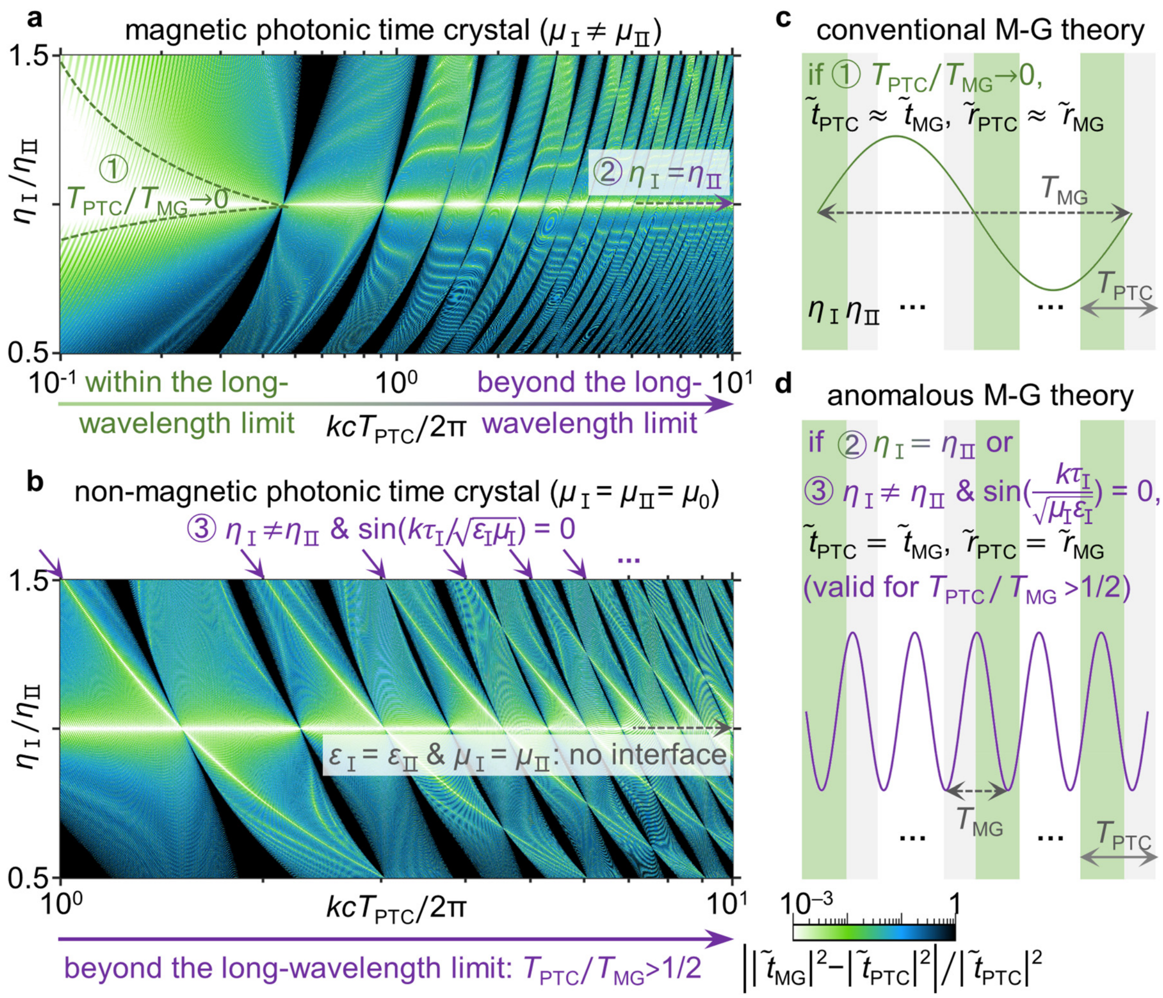

FIG. 3. Anomalous Maxwell-Garnett theory of light in the impedance-momentum parameter space. The photonic time crystal is surrounded by vacuum in the time domain and has a temporal interface number $N = 201$. (a) and (b) $\left||\tilde{t}_{\mathrm{MG}}|^2 - |\tilde{t}_{\mathrm{PTC}}|^2\right|/|\tilde{t}_{\mathrm{PTC}}|^2$ as a function of $\eta_{\mathrm{I}}/\eta_{\mathrm{II}}$ and $kcT_{\mathrm{PTC}}/2\pi$. The relative error $\left||\tilde{t}_{\mathrm{MG}}|^2 - |\tilde{t}_{\mathrm{PTC}}|^2\right|/|\tilde{t}_{\mathrm{PTC}}|^2$ is used to quantitively describe the accuracy of Maxwell-Garnett theory in the homogenization of photonic time crystals. For illustration, $\varepsilon_{\mathrm{I}}/\varepsilon_0 = 1$, $\varepsilon_{\mathrm{II}}/\varepsilon_0 = 2.1$, and $\mu_{\mathrm{II}}/\mu_0 = 1$ are used in (a), while $\varepsilon_{\mathrm{II}}/\varepsilon_0 = 2.1$ and $\mu_{\mathrm{I}}/\mu_0 = \mu_{\mathrm{II}}/\mu_0 = 1$ are used in (b). The temporal periods of photonic time crystals are the same as those in Fig. 2. For non-magnetic time crystals with $\eta_{\mathrm{I}}/\eta_{\mathrm{II}} = 1$ in (b), this trivial scenario directly corresponds to $\varepsilon_{\mathrm{I}} = \varepsilon_{\mathrm{II}}$ and $\mu_{\mathrm{I}} = \mu_{\mathrm{II}}$, indicating the absence of temporal interfaces inside the photonic time crystal. (c) and (d) Comparison between conventional and anomalous Maxwell-Garnett theories. The conventional Maxwell-Garnett theory works only within the long-wavelength regime in (c), namely, if $T_{\mathrm{PTC}}/T_{\mathrm{MG}} \to 0$. By contrast, the anomalous Maxwell-Garnett theory remains valid beyond the long-wavelength limit (e.g., $T_{\mathrm{PTC}}/T_{\mathrm{MG}} > 1/2$) in (d), either by exploiting the impedance matching or the Fabry–Pérot resonance.

by our finding that this anomalous Maxwell-Garnett theory of light might be extended to spatially inhomogeneous photonic crystals via the spatial Fabry–Pérot resonance, and that the analogous Maxwell-Garnett theory might exist in other wave systems, such as acoustic and water waves. Due to the mathematical simplicity and the physical elegance, our revealed anomalous Maxwell-Garnett theory of light may further stimulate the continuous exploration of more exotic light-matter interactions in temporal or spatiotemporal media,[55–60] particularly in systems involving moving free electrons[61–71] or complex dipolar sources.[72–78] For example, it is worthy to explore the potential interplay between our revealed anomalous Maxwell-Garnett theory beyond the long-wavelength limit and the breakdown of effective medium theory in the extreme subwavelength limit[22] in judiciously designed spatiotemporal media featuring both spatial and temporal interfaces,[48] where temporal total transmission and spatial total reflection might occur simultaneously. Moreover, our finding may intrigue the further exploration of many enticing open scientific questions that remain elusive, for example, the possible realization of broadband interfacial Cherenkov radiation from periodic structures. As background, the interfacial Cherenkov radiation,[65] as originating from the interaction between free electrons and periodic structures, provides a disruptive way to create the directional light emission at arbitrary frequencies and is vital for the development of many enticing on-chip applications, such as integrated light sources at previously hard-to-reach frequencies and miniaturized particle detectors

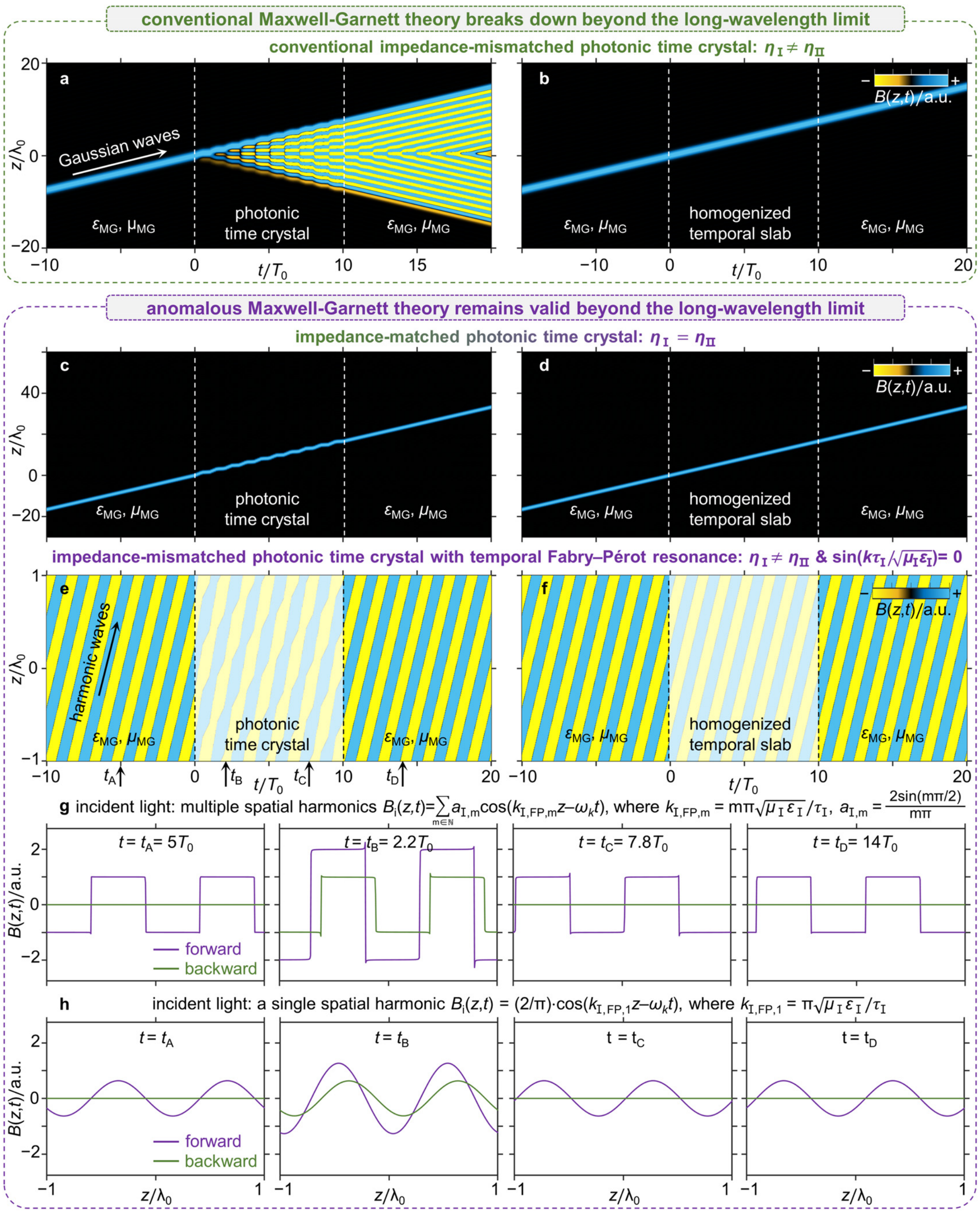

FIG. 4. Spatiotemporal evolution of space-time wave packets interacting with various photonic time crystals beyond the long-wavelength limit. For illustration, the photonic time crystal is surrounded by temporally semi-infinite media with the permittivity ε_{MG} and the permeability μ_{MG}. (a) and (b) The conventional Maxwell-Garnett theory breaks down beyond the long-wavelength limit. (c)–(h) The anomalous Maxwell-Garnett theory remains valid beyond the long-wavelength limit. The photonic time crystal is impedance-mismatched (i.e. $\eta_I \neq \eta_{II}$) in (a) and (e) but impedance-matched (i.e. $\eta_I = \eta_{II}$) in (c). Meanwhile, one constituent medium (e.g., medium I) in (e) satisfies the temporal Fabry–Pérot resonance condition, namely, $\sin(\omega_I\tau_I) = 0$. The wave packet' states before entering, traveling inside, and after exiting the impedance-mismatched photonic time crystal with the temporal Fabry–Pérot resonance in (e) are highlighted in (g) and (h). The incident wave packet follows a Gaussian waveform $B_i(z,t) = B(z,t<t_1) = \int_{-k_0}^{k_0} dk e^{-k^2/2\sigma_k^2} e^{ikz-i\omega t}$ in (a)–(d), a multiple-spatial-harmonic waveform $B_i(z,t) = B(z,t<t_1) = \sum_{m\in\mathbb{N}} a_{I,m}\cos(k_{I,FP,m}z-\omega_k t)$ in (e)–(g), and a single-spatial-harmonic waveform $B(z,t<t_1) = \cos(k_{I,FP,1}r-\omega_k t)$ in (h), where $\sigma_k = k_0/3$, $k_0 = 2\pi/\lambda_0 = 2\pi/cT_0$, $k_{I,FP,m} = m\pi\sqrt{\mu_I\varepsilon_I}/\tau_I$, $\omega_k = k/\sqrt{\mu\varepsilon}$, $a_{I,m} = \frac{2\sin(m\pi/2)}{m\pi}$, and $T_0 = T_{PTC}$. The photonic time crystals in (a),(c),(e) are the same as those in Figs. 2(b)–2(d), respectively, except that we set the interface number $N = 21$ here.

with enhanced sensitivity. However, the interfacial Cherenkov radiation severely suffers from the chromatic issue, due to the inherent structural dispersion of periodic structures. Whether it is possible to achieve the achromatic interfacial Cherenkov radiation from periodic structures via the anomalous Maxwell-Garnett theory of light is certainly worthy of in-depth exploration.

SUPPLEMENTARY MATERIAL

See the supplementary material for three sections, including rigorous proof for the accuracy of Maxwell-Garnett theory in predicting the transmission and reflection coefficients of photonic time crystals, analytical derivation for the spatiotemporal evolution of various wave packets interacting with photonic time crystals beyond the long-wavelength limit, and more discussion on anomalous Maxwell-Garnett theory for photonic time crystals.

ACKNOWLEDGMENTS

X.L. acknowledges the support partly from the Fundamental Research Funds for the Central Universities under Grant No. 226-2024-00022, the National Natural Science Fund for Excellent Young Scientists Fund Program (Overseas) of China, and the National Natural Science Foundation of China (NSFC) under Grant Nos. 62475227 and 62175212, and the Zhejiang Provincial Natural Science Fund Key Project under Grant No. LZ23F050003. H.C. acknowledges the support from the Key Research and Development Program of the Ministry of Science and Technology under Grant Nos. 2022YFA1404704, 2022YFA1405200, and 2022YFA1404902, the Key Research and Development Program of Zhejiang Province under Grant No. 2022C01036, and the Fundamental Research Funds for the Central Universities. R.C. acknowledges the support from the NSFC under Grant No. 623B2089.

AUTHOR DECLARATIONS

Conflict of Interest

The authors have no conflicts to disclose.

Author Contributions

Zheng Gong: Conceptualization (equal); Formal analysis (equal); Investigation (lead); Methodology (lead); Validation (equal); Visualization (lead); Writing – original draft (lead); Writing – review & editing (lead). **Ruoxi Chen:** Conceptualization (equal); Formal analysis (equal); Funding acquisition (equal); Validation (equal); Visualization (equal). **Hongsheng Chen:** Conceptualization (equal); Formal analysis (equal); Funding acquisition (equal); Methodology (equal); Supervision (equal); Validation (equal); Writing – review & editing (equal). **Xiao Lin:** Conceptualization (equal); Formal analysis (equal); Funding acquisition (equal); Methodology (equal); Supervision (equal); Validation (equal); Writing – original draft (equal); Writing – review & editing (lead).

DATA AVAILABILITY

The data that support the findings of this study are available within the article and its supplementary material.

REFERENCES

[1]T. C. Choy, *Effective Medium Theory: Principles and Applications* (Oxford University Press, 2015).
[2]V. A Markel, "Introduction to the Maxwell Garnett approximation: Tutorial," J. Opt. Soc. Am. A **33**, 1244 (2016).
[3]J. C. Maxwell-Garnett, "Colours in metal glasses and in metallic films," Philos. Trans. R. Soc. London, Ser. A **203**, 385 (1904).
[4]J. C Maxwell-Garnett, "Colours in metal glasses, in metallic films and in metallic solutions.—II," Philos. Trans. R. Soc. London, Ser. A **76**, 370 (1905).
[5]M. A. Biot, "Generalized theory of acoustic propagation in porous dissipative media," J. Acoust. Soc. Am. **34**, 1254 (1962).
[6]J. G Berryman, "Long-wavelength propagation in composite elastic media I. Spherical inclusions," J. Acoust. Soc. Am. **68**, 1809 (1980).
[7]C.-W. Nan, R. Birringer, D. R. Clarke, and H. Gleiter, "Effective thermal conductivity of particulate composites with interfacial thermal resistance," J. Appl. Phys. **81**, 6692 (1997).
[8]X. Hu and C. T. Chan, "Refraction of water waves by periodic cylinder arrays," Phys. Rev. Lett. **95**, 154501 (2005).
[9]J. Mei, Z. Liu, W. Wen, and P. Sheng, "Effective mass density of fluid-solid composites," Phys. Rev. Lett. **96**, 024301 (2006).
[10]Y. Liu and X. Zhang, "Metamaterials: A new frontier of science and technology," Chem. Soc. Rev. **40**, 2494 (2011).
[11]S. A. Cummer, J. Christensen, and A. Alù, "Controlling sound with acoustic metamaterials," Nat. Rev. Mater. **1**, 16001 (2016).
[12]K. Bertoldi, V. Vitelli, J. Christensen, and M. Van Hecke, "Flexible mechanical metamaterials," Nat. Rev. Mater. **2**, 17066 (2017).
[13]Y. Li, W. Li, T. Han, X. Zheng, J. Li, B. Li, S. Fan, and C.-W. Qiu, "Transforming heat transfer with thermal metamaterials and devices," Nat. Rev. Mater. **6**, 488 (2021).
[14]Y. Gelkop, F. Di Mei, S. Frishman, Y. Garcia, L. Falsi, G. Perepelitsa, C. Conti, E. DelRe, and A. J. Agranat, "Hyperbolic optics and superlensing in room-temperature KTN from self-induced k-space topological transitions," Nat. Commun. **12**, 7241 (2021).
[15]S. Kim, Y.-G. Peng, S. Yves, and A. Alù, "Loss compensation and superresolution in metamaterials with excitations at complex frequencies," Phys. Rev. X **13**, 041024 (2023).
[16]J. Soric, Y. Ra'di, D. Farfan, and A. Alù, "Radio-transparent dipole antenna based on a metasurface cloak," Nat. Commun. **13**, 1114 (2022).
[17]C. Wang, X. Chen, Z. Gong, R. Chen, H. Hu, H. Wang, Y. Yang, L. Tony, B. Zhang, and H. Chen, "Superscattering of light: Fundamentals and applications," Rep. Prog. Phys. **87**, 126401 (2024).
[18]S. Qu, Y. Hou, and P. Sheng, "Conceptual-based design of an ultrabroadband microwave metamaterial absorber," Proc. Natl. Acad. Sci. U.S.A. **118**, e2110490118 (2021).
[19]S. O'Brien and J. B. Pendry, "Photonic band-gap effects and magnetic activity in dielectric composites," J. Phys.: Condens. Matter **14**, 4035 (2002).
[20]T. Koschny, M. Kafesaki, E. N. Economou, and C. M. Soukoulis, "Effective medium theory of left-handed materials," Phys. Rev. Lett. **93**, 107402 (2004).
[21]V. Pacheco-Peña and N. Engheta, "Effective medium concept in temporal metamaterials," Nanophotonics **9**, 379 (2020).
[22]H. Herzig Sheinfux, I. Kaminer, Y. Plotnik, G. Bartal, and M. Segev, "Subwavelength multilayer dielectrics: Ultrasensitive transmission and breakdown of effective-medium theory," Phys. Rev. Lett. **113**, 243901 (2014).
[23]J. C. Serra and M. G. Silveirinha, "Homogenization of dispersive space-time crystals: Anomalous dispersion and negative stored energy," Phys. Rev. B **108**, 035119 (2023).
[24]M. V. Rybin, D. S. Filonov, K. B. Samusev, P. A. Belov, Y. S. Kivshar, and M. F. Limonov, "Phase diagram for the transition from photonic crystals to dielectric metamaterials," Nat. Commun. **6**, 10102 (2015).
[25]J. E. Sipe, P. Sheng, B. S. White, and M. H. Cohen, "Brewster anomalies: A polarization-induced delocalization effect," Phys. Rev. Lett. **60**, 108 (1988).
[26]P. A. Huidobro, M. G. Silveirinha, E. Galiffi, and J. B. Pendry, "Homogenization theory of space-time metamaterials," Phys. Rev. Appl. **16**, 014044 (2021).
[27]X. Chen, T. M. Grzegorczyk, B.-I. Wu, J. Pacheco, Jr., and J. A. Kong, "Robust method to retrieve the constitutive effective parameters of metamaterials," Phys. Rev. E **70**, 016608 (2004).

[28]D. R. Smith, S. Schultz, P. Markoš, and C. M. Soukoulis, "Determination of effective permittivity and permeability of metamaterials from reflection and transmission coefficients," Phys. Rev. B **65**, 195104 (2002).
[29]Y. Wu, J. Li, Z.-Q. Zhang, and C. T. Chan, "Effective medium theory for magnetodielectric composites: Beyond the long-wavelength limit," Phys. Rev. B **74**, 085111 (2006).
[30]S. Torquato and J. Kim, "Nonlocal effective electromagnetic wave characteristics of composite media: Beyond the quasistatic regime," Phys. Rev. X **11**, 021002 (2021).
[31]P. Garg, A. G. Lamprianidis, S. Rahman, N. Stefanou, E. Almpanis, N. Papanikolaou, B. Verfürth, and C. Rockstuhl, "Two-step homogenization of spatiotemporal metasurfaces using an eigenmode-based approach," Opt. Mater. Express **14**, 549 (2024).
[32]M. Lyubarov, Y. Lumer, A. Dikopoltsev, E. Lustig, Y. Sharabi, and M. Segev, "Amplified emission and lasing in photonic time crystals," Science **377**, 425 (2022).
[33]N. Engheta, "Four-dimensional optics using time-varying metamaterials," Science **379**, 1190 (2023).
[34]R. Won, "It's a matter of time," Nat. Photonics **17**, 209 (2023).
[35]T. Liu, J.-Y. Ou, K. F. MacDonald, and N. I. Zheludev, "Photonic metamaterial analogue of a continuous time crystal," Nat. Phys. **19**, 986 (2023).
[36]E. Galiffi, G. Xu, S. Yin, H. Moussa, Y. Ra'di, and A. Alù, "Broadband coherent wave control through photonic collisions at time interfaces," Nat. Phys. **19**, 1703 (2023).
[37]J. Kim, D. Lee, S. Yu, and N. Park, "Unidirectional scattering with spatial homogeneity using correlated photonic time disorder," Nat. Phys. **19**, 726 (2023).
[38]R. Tirole, S. Vezzoli, E. Galiffi, I. Robertson, D. Maurice, B. Tilmann, S. A. Maier, J. B. Pendry, and R. Sapienza, "Double-slit time diffraction at optical frequencies," Nat. Phys. **19**, 999 (2023).
[39]H. Moussa, G. Xu, S. Yin, E. Galiffi, Y. Ra'di, and A. Alù, "Observation of temporal reflection and broadband frequency translation at photonic time interfaces," Nat. Phys. **19**, 863 (2023).
[40]J. Sisler, P. Thureja, M. Y. Grajower, R. Sokhoyan, I. Huang, and H. A. Atwater, "Electrically tunable space-time metasurfaces at optical frequencies," Nat. Nanotechnol. **19**, 1491 (2024).
[41]X. Wang, P. Garg, M. S. Mirmoosa, A. G. Lamprianidis, C. Rockstuhl, and V. S. Asadchy, "Expanding momentum bandgaps in photonic time crystals through resonances," Nat. Photonics **19**, 149–155 (2025).
[42]C. Rizza, G. Castaldi, and V. Galdi, "Short-pulsed metamaterials," Phys. Rev. Lett. **128**, 257402 (2022).
[43]B. Apffel, S. Wildeman, A. Eddi, and E. Fort, "Experimental implementation of wave propagation in disordered time-varying media," Phys. Rev. Lett. **128**, 094503 (2022).
[44]Y. Pan, M.-I. Cohen, and M. Segev, "Superluminal k-gap solitons in nonlinear photonic time crystals," Phys. Rev. Lett. **130**, 233801 (2023).
[45]X. Wang, M. S. Mirmoosa, V. S. Asadchy, C. Rockstuhl, S. Fan, and S. A. Tretyakov, "Metasurface-based realization of photonic time crystals," Sci. Adv. **9**, eadg7541 (2023).
[46]J. E. Vázquez-Lozano and I. Liberal, "Incandescent temporal metamaterials," Nat. Commun. **14**, 4606 (2023).
[47]T. R. Jones, A. V. Kildishev, M. Segev, and D. Peroulis, "Time-reflection of microwaves by a fast optically-controlled time-boundary," Nat. Commun. **15**, 6786 (2024).
[48]L. Bar-Hillel, A. Dikopoltsev, A. Kam, Y. Sharabi, O. Segal, E. Lustig, and M. Segev, "Time refraction and time reflection above critical angle for total internal reflection," Phys. Rev. Lett. **132**, 263802 (2024).
[49]R. Yu and S. Fan, "Time-modulated near-field radiative heat transfer," Proc. Natl. Acad. Sci. U.S.A. **121**, e2401514121 (2024).
[50]Y. Ren, K. Ye, Q. Chen, F. Chen, L. Zhang, Y. Pan, W. Li, X. Li, L. Zhang, and H. Chen, "Observation of momentum-gap topology of light at temporal interfaces in a time-synthetic lattice," Nat. Commun. **16**, 707 (2025).
[51]M. Ciabattoni, Z. Hayran, and F. Monticone, "Observation of broadband super-absorption of electromagnetic waves through space-time symmetry breaking," Sci. Adv. **11**, eads7407 (2025).
[52]G. Ptitcyn, M. S. Mirmoosa, A. Sotoodehfar, and S. A. Tretyakov, "A tutorial on the basics of time-varying electromagnetic systems and circuits: Historic overview and basic concepts of time-modulation," IEEE Antennas Propag. Mag. **65**, 10 (2023).
[53]F. R. Morgenthaler, "Velocity modulation of electromagnetic waves," IRE Trans. Microwave Theory Tech. **6**, 167 (1958).
[54]J. A. Kong, *Electromagnetic Wave Theory* (EMW Publishing, 2008).
[55]E. Galiffi, R. Tirole, S. Yin, H. Li, S. Vezzoli, P. A. Huidobro, M. G. Silveirinha, R. Sapienza, A. Alù, and J. B. Pendry, "Photonics of time-varying media," Adv. Photonics **4**(1), 014002 (2022).
[56]J. Sloan, N. Rivera, J. D. Joannopoulos, and M. Soljacic, "Optical properties of dispersive time-dependent materials," ACS Photonics **11**, 950 (2024).
[57]G. Ptitcyn and N. Engheta, "Temporal twistronics," arXiv:2403.10477 (2024).
[58]A. Boltasseva, V. M. Shalaev, and M. Segev, "Photonic time crystals: From fundamental insights to novel applications: Opinion," Opt. Mater. Express **14**, 592 (2024).
[59]M. M. Asgari, P. Garg, X. Wang, M. S. Mirmoosa, C. Rockstuhl, and V. Asadchy, "Theory and applications of photonic time crystals: A tutorial," Adv. Opt. Photonics **16**, 958 (2024).
[60]W. Wu, Q. Chen, J.-D. Zhang, T. Huang, and D.-G. Fang, "Time modulated array antennas: A review," Electromagn. Sci. **2**, 1 (2024).
[61]A. Dikopoltsev, Y. Sharabi, M. Lyubarov, Y. Lumer, S. Tsesses, E. Lustig, I. Kaminer, and M. Segev, "Light emission by free electrons in photonic time-crystals," Proc. Natl. Acad. Sci. U.S.A. **119**, e2119705119 (2022).
[62]C. Roques-Carmes, S. E. Kooi, Y. Yang, N. Rivera, P. D. Keathley, J. D. Joannopoulos, S. G. Johnson, I. Kaminer, K. K. Berggren, and M. Soljačić, "Free-electron-light interactions in nanophotonics," Appl. Phys. Rev. **10**, 011303 (2023).
[63]J. Chen, R. Chen, Z. Gong, H. Hu, Y. Yang, X. Zhang, C. Wang, I. Kaminer, H. Chen, and B. Zhang, "Low-velocity-favored transition radiation," Phys. Rev. Lett. **131**, 113002 (2023).
[64]R. Chen, J. Chen, Z. Gong, X. Zhang, X. Zhu, Y. Yang, I. Kaminer, H. Chen, B. Zhang, and X. Lin, "Free-electron Brewster-transition radiation," Sci. Adv. **9**, eadh8098 (2023).
[65]Z. Gong *et al.*, "Interfacial Cherenkov radiation from ultralow-energy electrons," Proc. Natl. Acad. Sci. U.S.A. **120**, e2306601120 (2023).
[66]X. Gao, X. Zhao, X. Ma, and T. Dong, "Free electron emission in vacuum assisted by photonic time crystals," J. Phys. D: Appl. Phys. **57**, 315112 (2024).
[67]A. Balanov, A. Gorlach, V. Baryshevsky, I. Feranchuk, H. Nitta, Y. Hayakawa, A. Shchagin, Y. Takabayashi, Y. Danon, and L. J. Wong, "Coherent interactions of free electrons and matter: Toward tunable compact X-ray sources," arXiv:2412.15775 (2024).
[68]X. Shi, W. W. Lee, A. Karnieli, L. M. Lohse, A. Gorlach, L. W. W. Wong, T. Saldit, S. Fan, I. Kaminer, and L. J. Wong, "Quantum nanophotonics with energetic particles: X-rays and free electrons," arXiv:2411.09019 (2024).
[69]R. Ruimy, A. Karnieli, and I. Kaminer, "Free-electron quantum optics," Nat. Phys. **21**, 193 (2025).
[70]Z. Gong, R. Chen, Z. Wang, X. Xi, Y. Yang, B. Zhang, H. Chen, I. Kaminer, and X. Lin, "Free-electron resonance transition radiation via Brewster randomness," Proc. Natl. Acad. Sci. U.S.A. **122**, e2413336122 (2025).
[71]A. Nussupbekov, J.-F. Zhu, Y. Akimov, P. Bai, C. E. Png, F. J. Garcia-Vidal, and L. Wu, "Probing dynamics of time-varying media: Beyond abrupt temporal interfaces," arXiv: 2501.12899 (2025).
[72]C. Wang, Y. Zhong, X. Chen, H. Wang, T. Low, H. Chen, B. Zhang, and X. Lin, "Near-field coupling of Janus dipoles beyond polarization locking," Laser Photonics Rev. **18**, 2301035 (2024).
[73]Y. Cheng, K. A. Oyesina, B. Xue, D. Lei, A. M. H. Wong, and S. Wang, "Directional dipole dice enabled by anisotropic chirality," Proc. Natl. Acad. Sci. U.S.A. **120**, e2301620120 (2023).
[74]X. Chen, C. Wang, Y. Zhong, B. Zhang, H. Chen, and X. Lin, "Dipolar Huygens-Kerker radiation for surface waves," Opt. Lett. **49**, 4238 (2024).
[75]X. Shi, X. Lin, I. Kaminer, F. Gao, Z. Yang, J. D. Joannopoulos, M. Soljačić, and B. Zhang, "Superlight inverse Doppler effect," Nat. Phys. **14**, 1001 (2018).
[76]X. Lin and B. Zhang, "Normal Doppler frequency shift in negative refractive-index systems," Laser Photonics Rev. **13**, 1900081 (2019).
[77]S. Zhong, L. Qiao, X. Ge, X. Xu, Y. Fu, S. Gao, K. Zhanghao, H. Hao, W. Wang, and M. Li, "Three-dimensional dipole orientation mapping with high temporal-spatial resolution using polarization modulation," PhotoniX **5**, 19 (2024).
[78]T. Wu, A. B. Evlyukhin, and V. R. Tuz, "Separation of a toroidal mode in clusters of dielectric particles," Prog. Electromagn. Res. **180**, 103 (2024).